tial body weight, and then administered daily with MP (1,000 ppm; n = 20), CRB (300 ppm; n = 20), LMG (1,160 ppm; n = 20), BNF (10,000 ppm; n = 20) or OX (500 ppm; n= 20) in the basal diet, or with PMZ (100 mg/kg body weight) by gavage in 0.5% methyl cellulose (n = 22) for 7 or 28 days. Untreated controls (n = 20) were maintained on the basal diet and tap water without any treatment during the experimental period. After the 7 or 28 days of treatment, half (n = 10 or 20) of the animals in each group were euthanized by exsanguination from the abdominal aorta under deep anesthesia with CO_2/O_2, then their livers were removed.

In the administration experiment for 90 days, animals were divided into nine groups based on the initial body weight, and then administered daily with MP (1,000 ppm; n = 10), TAA (400 ppm; n = 10), CRB (300 ppm; n = 10), LMG (1,160 ppm; n = 10), BNF (10,000 ppm; n = 10), OX (500 ppm; n = 10) or APAP (10,000 ppm) in the basal diet (n = 10), or with PMZ (100 mg/kg body weight) by gavage in 0.5% methyl cellulose (n = 12) for 90 days. Untreated controls (n = 10) were maintained on the basal diet and tap water without any treatment during the experimental period. In the PMZ group, one animal died at day 63 after the start of treatment, because of an administration failure. After 90 days of treatment, animals in each group were euthanized by exsanguination from the abdominal aorta under deep anesthesia with CO_2/O_2, then their livers were removed.

The doses of MP, TAA and CRB have been shown to induce liver tumors in rats (Becker, 1983; King, 1976; NTP, 2000). The doses of BNF and OX have been shown to promote preneoplastic lesions as determined by glutathione *S*-transferase placental form in the liver after a 6-week administration in a two-stage model using rats (Mitsumori *et al.*, 1997; Shoda *et al.*, 2000). The doses of LMG, APAP and PMZ induced hepatotoxicity after a 28-day or 13-week administration in rats (NTP, 1993a, 1993b, 2005).

All animal experiments were conducted in accordance with the "Guidelines for Proper Conduct of Animal Experiments" (Science Council of Japan, June 1, 2006), and the animal protocols were reviewed and approved by the Animal Care and Use Committee of the Tokyo University of Agriculture and Technology. All efforts were made to minimize animal suffering.

Histology and immunohistochemistry

Three-micrometer sections of paraffin-embedded liver tissues were stained with hematoxylin and eosin for histopathological examination, or subjected to immunohistochemistry. Immunohistochemistry of liver sections was performed using the Vectastain® Elite ABC Kit (Vector Laboratories Inc., Burlingame, CA, USA) with 3,3'-diaminobenzidine/H_2O_2 as the chromogen and the following antibodies: Ki-67, a marker of cell proliferation expressed in the nucleus during the G_1 to M phase of the cell cycle (Scholzen and Gerdes, 2000), phosphorylated Histone H3 (p-Histone H3), acting on chromosome condensation at the early M phase (Hirota *et al.*, 2005), topoisomerase II alpha (TOP2A), acting on DNA decatenation in G_2/M phase (Mattila *et al.*, 2007), $p21^{Cip1}$, one of the cyclin-dependent kinase inhibitors acting in G_1/S phase (Sherr and Roberts, 1995), UBD, a molecule that leads to chromosomal instability through reduction in kinetochore localization of checkpoint proteins, such as MAD2, during the G_2/M phase (Herrmann *et al.*, 2007; Lim *et al.*, 2006), p-MDM2, a p53 downstream molecule that facilitates degradation of p53 (Malmlöf *et al.*, 2007; Mayo and Donner, 2002), and cleaved caspase 3, an apoptosis marker expressed during the later stage of apoptosis (Eckle *et al.*, 2004). Antigen retrieval conditions and the concentration of each antibody are shown in Table 1. Immunostained sections were counterstained with hematoxylin for microscope examination. Endogenous peroxidase activity was blocked with 0.3% hydrogen peroxide.

In the double immunohistochemistry of UBD and TOP2A or p-Histone H3, 3,3'-diaminobenzidine was used to visualize UBD with the Vectastain® Elite ABC kit (Vector Laboratories Inc.), and Vector Red Alkaline Phosphate Substrate Kit I (Vector Laboratories Inc.) was used to visualize TOP2A and p-Histone H3 with the Vectastain® ABC-AP kit (Vector Laboratories Inc.).

Analysis of immunoreactivity

Cells immunoreactive to Ki-67, p-Histone H3, TOP2A, UBD, $p21^{Cip1}$ and p-MDM2 were counted in 10 randomly selected areas per animal at 200 × magnification, and cells immunoreactive to cleaved caspase 3 were counted in five randomly selected areas per animal at 100 × magnification, avoiding areas of connective tissues and vasculature. In the case of uneven immunoreactive cell distribution within the liver lobules, such as accumulation of immunoreactive cells at the periportal area, we selected five or 10 adjacent areas for analysis, to avoid disproportionate selection of areas. Immunoreactive liver cells were counted visually, and the total number of liver cells in the micrographs was separately counted using the image binarization method in the Win-ROOF image analysis and measurement software (version 6.4.2., Mitani Corporation, Fukui, Japan). Then, the percentage of total immunoreactive cells was estimated in each animal.

Table 1. Antibodies used for immunohistochemistry.

Antigen	Abbreviated name	Host species	Clone name	Dilution	Antigen retrieval	Manufacturer (City, State, Country)
Cleaved caspase 3 (Asp175)	-	Rabbit	Polyclonal	1:500	Autoclaving in target retrieval solution	Cell Signaling Technology, Inc. (Danvers, MA, USA)
Ki-67 antigen	Ki-67	Mouse	Monoclonal (MIB-5)	1:200	Autoclaving in citrate buffer	Dako (Glostrup, Denmark)
Phosphorylated histone H3 (Ser10)	Phospho-Histone H3	Rabbit	Polyclonal	1:400	Autoclaving in citrate buffer	Santa Cruz Biotechnology, Inc. (Santa Cruz, CA, USA)
Phosphorylated MDM2 (Ser166)	p-MDM2	Rabbit	Polyclonal	1:400	Autoclaving in target retrieval solution	Cell Signaling Technology, Inc.
$p21^{Cip1}$	-	Mouse	Monoclonal (CP74)	1:1000	Microwaving in citrate buffer	Abcam (Cambridge, UK)
Topoisomerase II alpha	TOP2A	Rabbit	Monoclonal (EP1102Y)	1:400	Autoclaving in citrate buffer	Epitomics, Inc. (Burlingame, CA, USA)
Ubiquitin D	UBD	Rabbit	Polyclonal	1:400	Autoclaving in citrate buffer	Proteintech Group, Inc. (Chicago, IL, USA)

Antigen retrieval was applied for immunohistochemistry. Retrieval conditions were either autoclaving at 121°C for 10 min in 10 mM citrate buffer (pH 6.0) or in target retrieval solution (3-in-1; pH 9.0, Dako), or microwaving at 90°C for 10 min in 10 mM citrate buffer (pH 6.0).

Table 2. Sequence of primers used for real-time RT-PCR.

Gene	Accession no.	Forward primer (5'→3')	Reverse primer (5'→3')
Cdkn1a	NM_080782	ACCAGCCACA GGCACCAT	CGGCATACTT TGCTCCTGTG T
Chek1	NM_080400	TGGCAGCTGG CAAAGGA	AATCCCAGTC TTCCACAAAA GG
Mad2l1	NM_001106594	ACAGCCACTG TGACATTTCT ACCA	CCCGATTCTT CCCACTTTTC A
Mdm2	NM_001108099	GAAGGAGGAC ACACAAGACA AAGA	ATGGCTCGAT GGCGTTCA
Rbl2	NM_031094	AAGTGAATCG CCTGCAAAAA G	CTCGGTCATT AGCTACATCT TGGA
Tp53	NM_030989	CATGAGCGTT GCTCTGATGG T	GATTTCCTTC CACCCGGATA A
Housekeeping genes			
Actb	NM_031144	CCCTGGCTCC TAGCACCAT	AGAGCCACCA ATCCACACAG A
Hprt1	NM_012583	GCCGACCGGT TCTGTCAT	TCATAACCTG GTTCATCATC ACTAATC

Abbreviations: *Actb*, actin, beta; *Cdkn1a*, cyclin-dependent kinase inhibitor 1A; *Chek1*, checkpoint kinase 1; *Hprt1*, hypoxanthine phosphoribosyltransferase 1; *Mad2l1*, MAD2 mitotic arrest deficient-like 1 (yeast); *Mdm2*, MDM2 proto-oncogene, E3 ubiquitin protein ligase; *Rbl2*, retinoblastoma-like 2; RT-PCR, reverse transcription polymerase chain reaction; *Tp53*, tumor protein p53.

Real-time RT-PCR analysis

To investigate the expression levels of representative cell cycle-related genes in the liver, mRNA expression analysis was performed using the StepOnePlus™ Real-time RT-PCR System (Life Technologies, Carlsbad, CA, USA) with the SYBR®Green PCR Master Mix (Life Technologies). The forward and reverse primers listed in Table 2 were designed using the Primer Express 3.0 software (Life Technologies). Using the threshold cycle values of hypoxanthine phosphoribosyl transferase 1 (*Hprt1*) or actin, beta (*Actb*) in the same sample as the endogenous control, the relative differences in gene expression were

Table 3. Initial and final body weight and liver weight of rats after treatment with hepatocarcinogens, hepatocarcinogenic promoters or non-carcinogenic hepatotoxicants.

Group	Number of animals	Initial body weight (g)	Final body weight (g)	Liver weight	
				Absolute (g)	Relative (g/100g BW)
Day 7					
CONT	10	119.1 ± 4.7	161.9 ± 6.8	7.26 ± 0.35	4.49 ± 0.10
MP	10	118.9 ± 4.1	150.4 ± 5.0**	7.39 ± 0.43	4.91 ± 0.14**
CRB	10	118.9 ± 4.5	152.1 ± 4.9**	7.17 ± 0.34	4.72 ± 0.20*
LMG	10	119.0 ± 4.7	149.7 ± 3.7**	8.76 ± 0.35**	5.85 ± 0.22**
BNF	10	117.4 ± 2.9	154.6 ± 6.9**	8.05 ± 0.41**	5.21 ± 0.28**
OX	10	120.1 ± 4.2	162.8 ± 4.6	8.71 ± 0.40**	5.35 ± 0.23**
PMZ	11	117.1 ± 3.0	134.3 ± 5.2**	6.89 ± 0.41	5.13 ± 0.25**
Day 28					
CONT	10	119.9 ± 9.4	252.6 ± 13.2	10.47 ± 0.82	4.15 ± 0.26
MP	10	119.4 ± 8.6	176.2 ± 9.1**	7.54 ± 0.49**	4.28 ± 0.20
CRB	10	120.4 ± 7.3	230.7 ± 10.6**	10.07 ± 0.63	4.36 ± 0.14**
LMG	10	119.1 ± 7.9	216.4 ± 9.0**	12.00 ± 0.66**	5.55 ± 0.25**
BNF	10	117.4 ± 8.2	230.3 ± 10.0**	11.37 ± 0.76**	4.94 ± 0.19**
OX	10	118.7 ± 6.9	238.8 ± 8.0**	12.41 ± 0.71**	5.20 ± 0.17**
PMZ	11	117.4 ± 6.6	192.5 ± 8.8**	10.16 ± 0.54	5.28 ± 0.18**
Day 90					
CONT	10	134.5 ± 8.5	351.8 ± 30.6	11.04 ± 1.37	3.13 ± 0.13
MP	10	134.3 ± 8.0	236.2 ± 18.2**	7.95 ± 0.85**	3.36 ± 0.14*
TAA	10	133.5 ± 7.5	223.9 ± 8.8**	11.18 ± 0.81	4.99 ± 0.23**
CRB	10	131.7 ± 6.4	302.1 ± 13.7**	11.43 ± 0.50	3.79 ± 0.16**
LMG	10	132.2 ± 6.3	293.1 ± 12.0**	13.04 ± 0.70**	4.45 ± 0.19**
BNF	10	133.6 ± 7.0	324.7 ± 8.9*	13.08 ± 0.72**	4.03 ± 0.14**
OX	10	132.4 ± 6.7	348.9 ± 14.0	14.84 ± 0.96**	4.26 ± 0.26**
APAP	10	131.2 ± 6.4	327.1 ± 12.6*	12.01 ± 0.76*	3.67 ± 0.18**
PMZ	11	131.6 ± 6.9	277.8 ± 8.6**	13.75 ± 0.53**	4.95 ± 0.22**

Abbreviations: APAP, acetaminophen; BNF, β-naphthoflavone; CONT, untreated controls; CRB, carbadox; LMG, leucomalachite green; MP, methapyrilene; OX, oxfendazole; PMZ, promethazine; TAA, thioacetamide. Values are expressed as mean ± S.D. * $P < 0.05$, ** $P < 0.01$ vs. untreated controls (Dunnett's or Steel's test).

calculated using the $2^{-\Delta\Delta C_T}$ method (Livak and Schmittgen, 2001).

Statistical analysis

All data are represented as mean ± S.D. Numerical data were analyzed by the Bartlett's test for the homogeneity of variance. If there was no significant difference in variance, Dunnett's test was performed for comparison between the groups. If a significant difference was found in variance, Steel's test was performed. All numerical data of the treatment groups were compared with those of untreated controls.

RESULTS

Body and liver weight

At day 7, the final body weight significantly decreased in the MP, CRB, LMG, BNF and PMZ groups, compared with the untreated controls (Table 3). The absolute liver weight of rats in the LMG, BNF and OX groups was sig-

nificantly higher than that of the untreated controls. The relative liver weight of rats in all treated groups was significantly higher than that of the untreated controls.

At day 28, the final body weight significantly decreased in all treated groups, compared with the untreated controls (Table 3). The absolute liver weight of rats in the MP group was significantly lower than that of the untreated controls. However, the absolute liver weight of rats in the LMG, BNF and OX groups was significantly higher than that of the untreated controls. The relative liver weight of rats in the CRB, LMG, BNF, OX and PMZ groups was significantly higher than that of the untreated controls.

At day 90, the final body weight significantly decreased in the MP, TAA, CRB, LMG, BNF, APAP and PMZ groups, compared with the untreated controls (Table 3). The absolute liver weight of rats in the MP group was significantly lower than that of the untreated controls. However, the absolute liver weight of rats in the LMG, BNF, OX, APAP and PMZ groups was significantly higher than that of the untreated controls. The relative liver weight of rats in all treated groups was significantly higher than that of the untreated controls.

Histopathological changes

MP treatment revealed diffused liver cell cytomegaly that was often associated with anisokaryosis, aberrant mitosis and apoptosis at all time points, as previously reported (NTP, 2000). Bile duct proliferation, oval cell proliferation accompanied with mild interstitial fibrosis and pigmentation were evident in the periportal area at day 28 and day 90. In addition, cholangiofibrosis and eosinophilic liver cell foci were scattered at day 90. Treatment with CRB revealed no apparent histological changes at all time points. LMG treatment resulted in centrilobular liver cell hypertrophy at all time points, as previously reported (NTP, 2005). Furthermore, liver cell fatty degeneration was scattered at day 90. Treatment with BNF revealed no apparent histological changes at day 7. At day 28 and day 90, centrilobular liver cell hypertrophy developed as previously reported (Shoda *et al.*, 2000). Moreover, liver cell fatty degeneration was scattered at day 90. OX treatment resulted in centrilobular hepatocellular hypertrophy and fatty degeneration at all time points, as previously reported (Mitsumori *et al.*, 1997). PMZ treatment resulted in centrilobular liver cell hypertrophy at all time points, as previously reported (NTP, 1993b). Additionally, liver cell fatty degeneration was scattered. TAA treatment revealed diffused liver cell cytomegaly that was often associated with anisokaryosis, aberrant mitosis and apoptosis at day 90, as previously reported (Becker, 1983). Bile duct proliferation, oval cell proliferation accompanied with mild interstitial fibrosis and pigmentation were observed in the periportal area. TAA treatment for 90 days also induced regenerating nodules with bundles of collagen surrounding the lobules. Treatment with APAP revealed no apparent histological changes at day 90.

Immunoreactive cellular distribution

Ki-67, p-Histone H3, TOP2A, $p21^{Cip1}$, p-MDM2 and cleaved caspase 3 were immunolocalized in the nucleus of liver cells, and UBD was immunolocalized in the cytoplasm or mitotic spindle of liver cells (Fig. 1A-G). Cells immunoreactive to Ki-67, p-Histone H3, TOP2A and UBD were distributed evenly within the liver lobules, except for preferential distribution in the periportal area in the PMZ group at day 28. Cells immunoreactive to $p21^{Cip1}$, p-MDM2 and cleaved caspase 3 were preferentially distributed in the periportal area in any group at any time point.

At day 7, the number of $Ki\text{-}67^+$ cells significantly increased in the MP group, and significantly decreased in the CRB, LMG and OX groups, compared with the untreated controls (Fig. 1A). The number of p-Histone $H3^+$ cells significantly decreased in the CRB and OX groups, compared with the untreated controls (Fig. 1B). The number of $TOP2A^+$ cells significantly increased in the MP group, and significantly decreased in the CRB and OX groups, compared with the untreated controls (Fig. 1C). The number of UBD^+ cells significantly increased in the MP group, and significantly decreased in the CRB, LMG and OX groups, compared with the untreated controls (Fig. 1D). The number of $p21^{Cip1+}$ cells significantly increased in the MP, CRB and LMG groups, compared with the untreated controls (Fig. 1E). The number of $p\text{-}MDM2^+$ cells significantly increased in the MP, LMG, BNF and PMZ groups, compared with the untreated controls (Fig. 1F). The number of cleaved caspase 3^+ cells significantly increased in the MP group, compared with the untreated controls (Fig. 1G).

At day 28, the number of $Ki\text{-}67^+$ cells significantly increased in the MP and PMZ groups, compared with the untreated controls (Fig. 2A). The number of p-Histone $H3^+$ cells significantly increased in the MP and PMZ groups, compared with the untreated controls (Fig. 2B). The number of $TOP2A^+$ cells significantly increased in the MP group, and significantly decreased in the CRB group, compared with the untreated controls (Fig. 2C). The number of UBD^+ cells significantly increased in the MP and PMZ groups, and significantly decreased in the CRB group, compared with the untreated controls (Fig. 2D). The number of $p21^{Cip1+}$ cells significantly increased in the CRB group, compared with the untreated

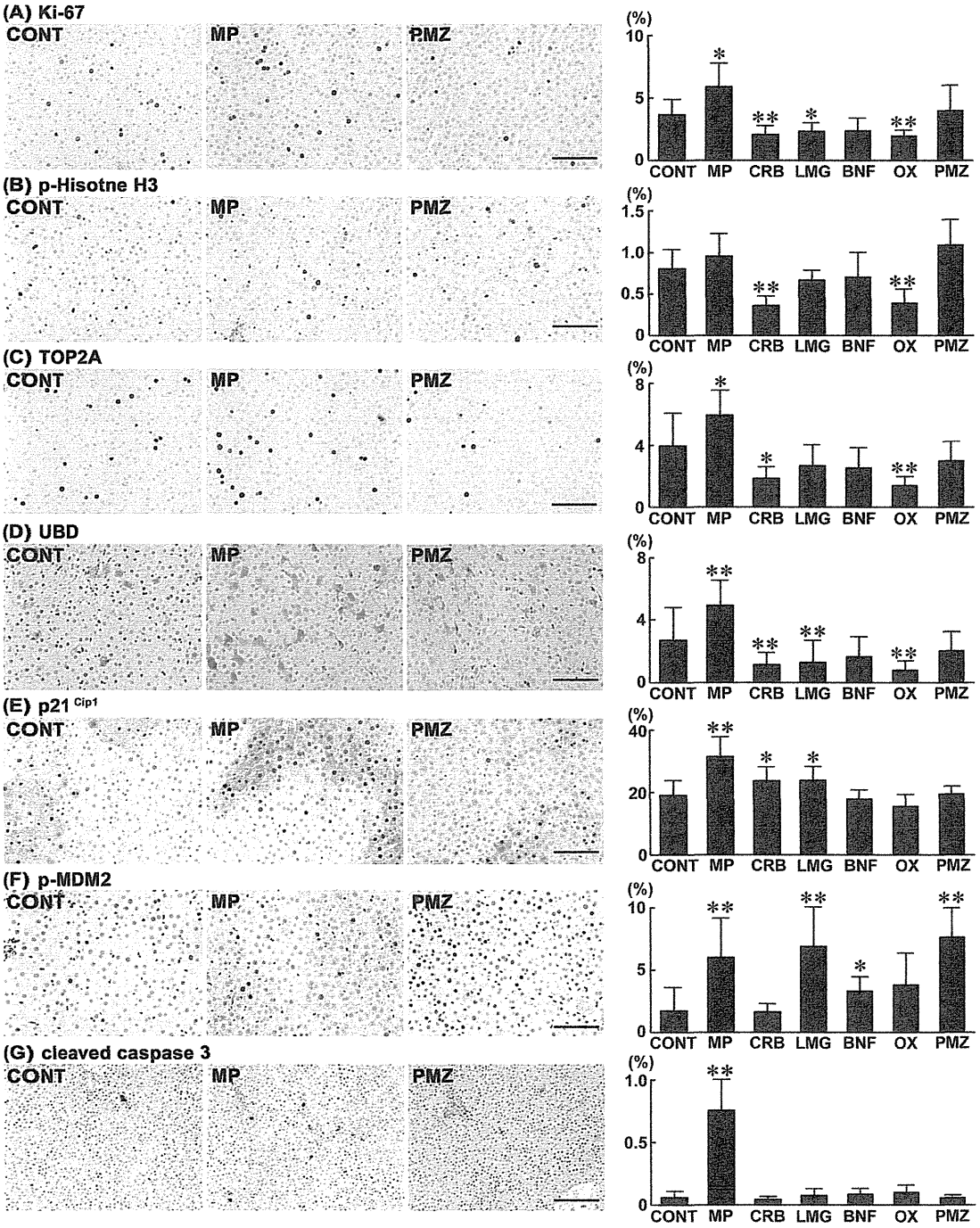

Fig. 1. Distribution of Ki-67+, p-Histone H3+, TOP2A+, UBD+, p21Cip1+, p-MDM2+ and cleaved caspase 3+ cells in the liver of rats at day 7 after treatment with hepatocarcinogens, hepatocarcinogenic promoters or non-carcinogenic hepatotoxicants. Photomicrographs show the distribution of Ki-67+, p-Histone H3+, TOP2A+, UBD+, p21Cip1+, p-MDM2+ and cleaved caspase 3+ cells in the liver of representative cases from untreated controls and animals treated with MP or PMZ. The graphs show positive cell ratios of hepatocytes per total cells counted in 10 animals of each group. Values represent mean + S.D. (A) Ki-67, (B) p-Histone H3, (C) TOP2A, (D) UBD, (E) p21Cip1+, (F) p-MDM2, and (G) cleaved caspase 3. Bar = 100 μm (A-F) or 200 μm (G). * $P < 0.05$, ** $P < 0.01$ vs. untreated controls (Dunnett's or Steel's test).

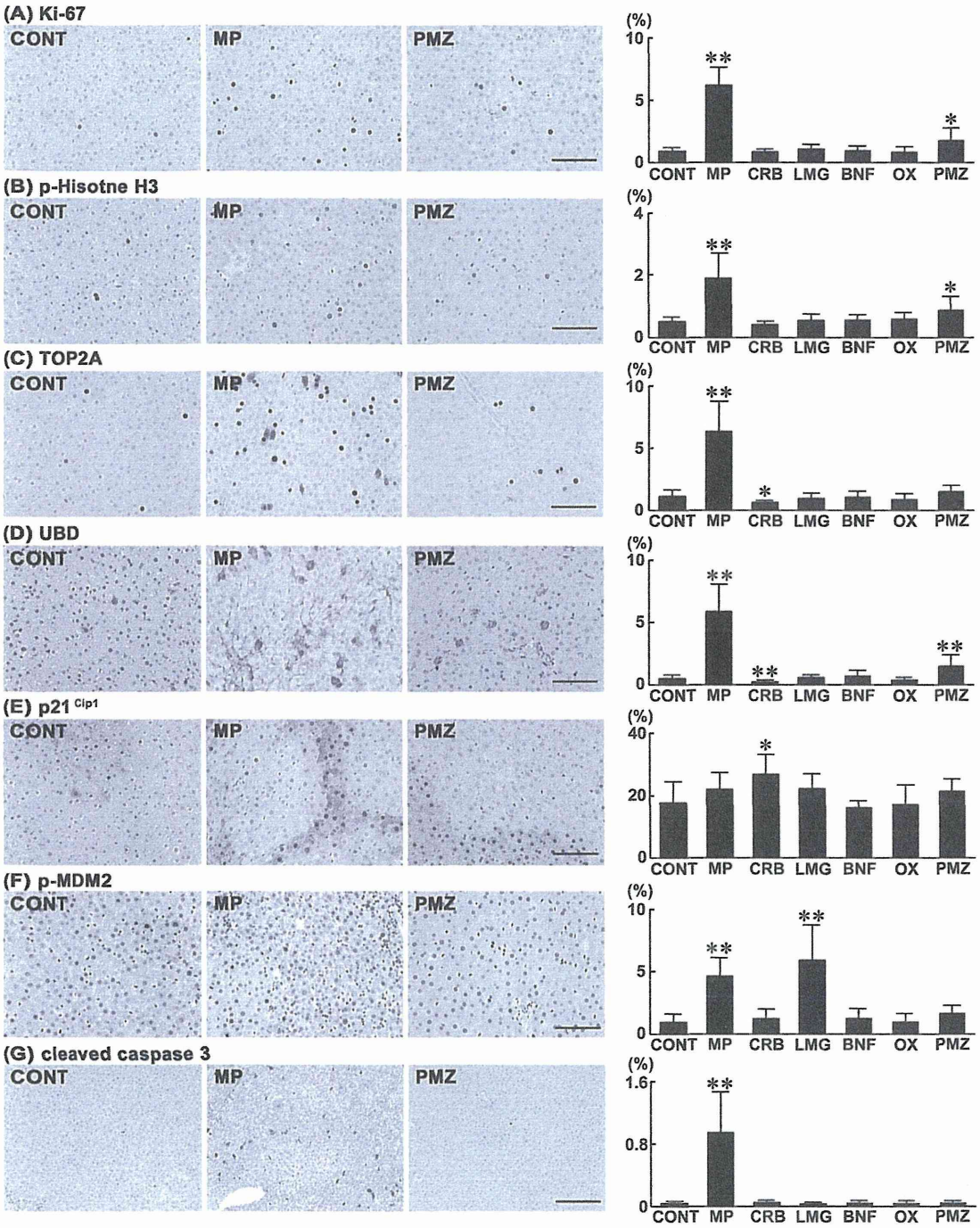

Fig. 2. Distribution of Ki-67$^+$, p-Histone H3$^+$, TOP2A$^+$, UBD$^+$, p21^{Cip1+}, p-MDM2$^+$ and cleaved caspase 3$^+$ cells in the liver of rats at day 28 after treatment with hepatocarcinogens, hepatocarcinogenic promoters or non-carcinogenic hepatotoxicants. Photomicrographs show the distribution of Ki-67$^+$, p-Histone H3$^+$, TOP2A$^+$, UBD$^+$, p21^{Cip1+}, p-MDM2$^+$ and cleaved caspase 3$^+$ cells in the liver of representative cases from untreated controls and animals treated with MP or PMZ. The graphs show positive cell ratios of hepatocytes per total cells counted in 10 animals of each group. Values represent mean + S.D. (A) Ki-67, (B) p-Histone H3, (C) TOP2A, (D) UBD, (E) p21^{Cip1+}, (F) p-MDM2, and (G) cleaved caspase 3. Bar = 100 μm (A-F) or 200 μm (G). * $P < 0.05$, ** $P < 0.01$ vs. untreated controls (Dunnett's or Steel's test).

controls (Fig. 2E). The number of p-MDM2$^+$ cells significantly increased in the MP and LMG groups, compared with the untreated controls (Fig. 2F). The number of cleaved caspase 3$^+$ cells significantly increased in the MP group, compared with the untreated controls (Fig. 2G).

At day 90, the number of Ki-67$^+$ cells significantly increased in the MP and TAA groups, compared with the untreated controls (Fig. 3A). The number of p-Histone H3$^+$ cells significantly increased in the MP and TAA groups, and significantly decreased in the CRB and APAP groups, compared with the untreated controls (Fig. 3B). The number of TOP2A$^+$ cells significantly increased in the MP and TAA groups, compared with the untreated controls (Fig. 3C). The number of UBD$^+$ cells significantly increased in the MP and TAA groups, compared with the untreated controls (Fig. 3D). The number of p21^{Cip1+} cells significantly increased in the TAA, CRB, LMG, OX, APAP and PMZ groups, compared with the untreated controls (Fig. 3E). The number of p-MDM2$^+$ cells significantly increased in the TAA and LMG groups, and significantly decreased in the OX group, compared with the untreated controls (Fig. 3F). The number of cleaved caspase 3$^+$ cells significantly increased in the MP, TAA and OX groups, compared with the untreated controls (Fig. 3G).

p-Histone H3$^+$/Ki-67$^+$ cell ratio

To estimate the population of proliferative cells existing at M phase, the ratio in the number of p-Histone H3$^+$ cells to that of Ki-67$^+$ cells was calculated using the data counted in immunohistochemical liver slides of each molecule in the same animal.

At day 7, the ratio of the number of p-Histone H3$^+$ cells to that of Ki-67$^+$ cells did not change in any of the treatment groups, compared with the untreated controls (Fig. 4A). At day 28, this ratio significantly decreased in the MP group, compared with the untreated controls (Fig. 4B). At day 90, the ratio of the number of p-Histone H3$^+$ cells to that of Ki-67$^+$ cells significantly decreased in the MP, TAA and CRB groups, compared with the untreated controls (Fig. 4C).

Double immunohistochemistry of UBD and TOP2A or p-Histone H3

At day 28, the number of UBD$^+$ cells within the population of the TOP2A$^+$ cells significantly increased in the MP and PMZ groups, compared with the untreated controls (Fig. 5A). In contrast, the ratio of the TOP2A$^+$ cells to the total number of UBD$^+$ cells did not change in any of the treatment groups. The number of UBD$^+$ cells within the population of p-Histone H3$^+$ cells significantly increased in the MP group, and significantly decreased in the CRB group, compared with the untreated controls (Fig. 5B). Furthermore, the ratio of the p-Histone H3$^+$ cells to the total number of UBD$^+$ cells significantly decreased in the MP group, compared with the untreated controls.

At day 90, the number of UBD$^+$ cells within the population of TOP2A$^+$ cells did not change in any of the treatment groups (Fig. 5C). In contrast, the ratio of the TOP2A$^+$ cells to the total number of UBD$^+$ cells significantly decreased in the MP group. The number of UBD$^+$ cells within the population of p-Histone H3$^+$ cells significantly decreased in the OX group, compared with the untreated controls (Fig. 5D). Furthermore, the ratio of the p-Histone H3$^+$ cells to the total number of UBD$^+$ cells significantly decreased in the MP and CRB groups, compared with the untreated controls.

Real-time RT-PCR analysis

Transcript levels of the genes listed in Table 2 at days 28 and 90 were determined by real-time RT-PCR in the MP, CRB, OX and PMZ groups, and compared with the levels in the untreated controls (Table 4).

At day 28, the transcript level of *Cdkn1a* after normalization against *Hprt1* and *Actb* levels significantly increased in the CRB group, and significantly decreased in the PMZ group, compared with the untreated controls. The transcript levels of *Chek1* after normalization against *Hprt1* and/or *Actb* significantly increased in the MP, OX and PMZ groups, compared with the untreated controls. The transcript levels of *Mad2l1* after normalization against *Hprt1* and *Actb* significantly increased in the MP and PMZ groups, compared with the untreated controls. The transcript levels of *Mad2l1* after normalization against *Hprt1* significantly decreased in the OX group, compared with the untreated controls. The transcript level of *Mdm2* after normalization against *Hprt1* and *Actb* significantly increased in the MP, CRB and OX groups, compared with the untreated controls. The transcript level of *Rbl2* after normalization against *Hprt1* and *Actb* significantly decreased in the MP group, compared with the untreated controls. The transcript level of *Rbl2* after normalization against *Actb* significantly increased in the CRB group, compared with the untreated controls. The transcript level of *Tp53* after normalization against *Hprt1* and/or *Actb* significantly increased in the MP and OX groups, compared with the untreated controls.

At day 90, the transcript level of *Cdkn1a* after normalization against *Hprt1* and *Actb* levels significantly increased in the CRB group, and significantly decreased in the PMZ group, compared with the untreated controls.

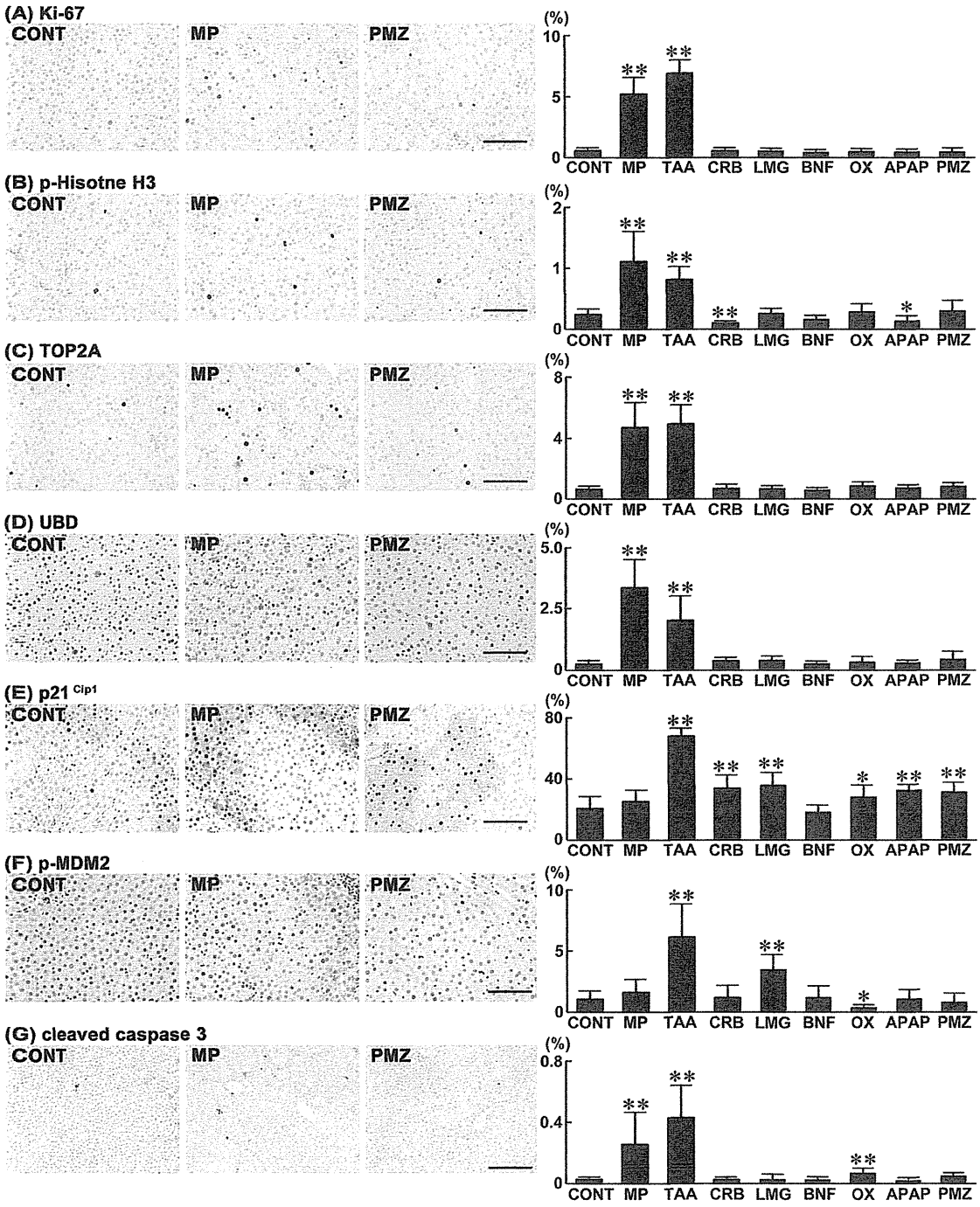

Fig. 3. Distribution of Ki-67$^+$, p-Histone H3$^+$, TOP2A$^+$, UBD$^+$, p21^{Cip1+}, p-MDM2$^+$ and cleaved caspase 3$^+$ cells in the liver of rats at day 90 after treatment with hepatocarcinogens, hepatocarcinogenic promoters or non-carcinogenic hepatotoxicants. Photomicrographs show the distribution of Ki-67$^+$, p-Histone H3$^+$, TOP2A$^+$, UBD$^+$, p21^{Cip1+}, p-MDM2$^+$ and cleaved caspase 3$^+$ cells in the liver of representative cases from untreated controls and animals treated with MP or PMZ. The graphs show positive cell ratios of hepatocytes per total cells counted in 10 animals of each group. Values represent mean + S.D. (A) Ki-67, (B) p-Histone H3, (C) TOP2A, (D) UBD, (E) p21^{Cip1+}, (F) p-MDM2, and (G) cleaved caspase 3. Bar = 100 μm (A-F) or 200 μm (G). * $P < 0.05$, ** $P < 0.01$ vs. untreated controls (Dunnett's or Steel's test).

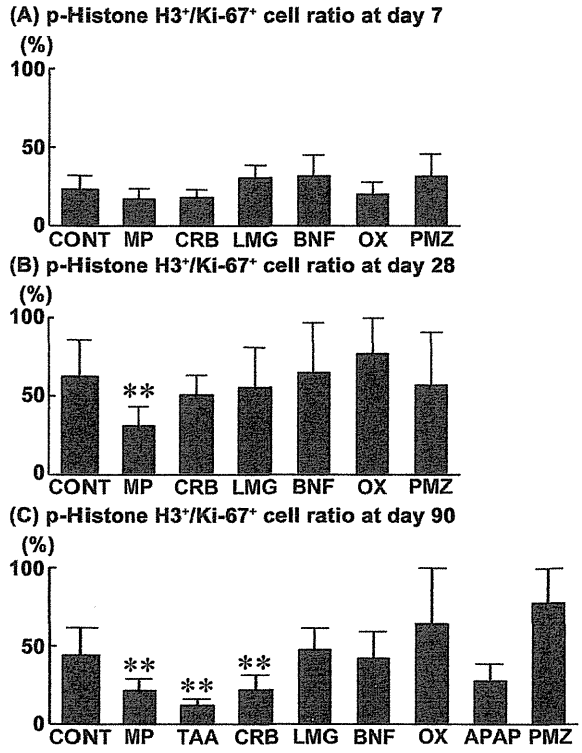

Fig. 4. p-Histone H3+/Ki-67+ cell ratio in the liver of rats at days 7, 28 and 90 after treatment with hepatocarcinogens, hepatocarcinogenic promoters and non-carcinogenic hepatotoxicants. The graphs show the p-Histone H3+ cell ratio of hepatocytes per number of Ki-67+ cells counted in 10 animals of each group. Values represent mean + S.D. (A) p-Histone H3+/Ki-67+ cell ratio at day 7, (B) p-Histone H3+/Ki-67+ cell ratio at day 28, and (C) p-Histone H3+/Ki-67+ cell ratio at day 90. ** $P < 0.01$ vs. untreated controls (Steel's test).

The transcript levels of *Chek1* and *Mad2l1* after normalization against *Hprt1* and *Actb* significantly increased in the MP group, compared with the untreated controls. The transcript level of *Chek1* after normalization against *Hprt1* significantly decreased in the OX group, compared with the untreated controls. The transcript level of *Mdm2* after normalization against *Hprt1* and/or *Actb* significantly increased in the MP and CRB groups, compared with the untreated controls. The transcript level of *Rbl2* after normalization against *Hprt1* and/or *Actb* significantly decreased in the MP and PMZ groups, compared with the untreated controls. The transcript level of *Tp53* after normalization against *Hprt1* significantly increased in the MP group, and significantly decreased in the OX group, compared with the untreated controls.

DISCUSSION

In our previous short time course study of up to 28 days using rats, we have shown hepatocarcinogen-specific cellular responses suggestive of disruption in G_1/S checkpoint and spindle checkpoint functions, as well as facilitation of cell proliferation and apoptosis at day 28 after starting administration, while no carcinogen-specific responses were observed at days 3 and 7 (Kimura *et al.*, 2015). In the present study, the hepatocarcinogen, MP, facilitated cell proliferation and increased cell populations expressing cell cycle-related molecules and apoptosis marker at days 7 and 28 after starting administration. However, MP did not decrease the p-Histone H3+ cell ratio within the Ki-67+ proliferating population at day 7, suggesting there was no disruption in spindle checkpoint function at this time point. Moreover, although hepatocarcinogens/promoters increased the number of p-MDM2+ cells at day 7 of administration, non-carcinogenic hepatotoxicant also increased the number of p-MDM2+ cells, suggestive of a cellular response unrelated to the carcinogenic mechanism. Therefore, these results suggest that it takes at least 28 days to induce hepatocarcinogen-specific cellular responses.

Here, we observed an increase in the number of Ki-67+, p-Histone H3+, TOP2A+, UBD+ and cleaved caspase 3+ cells by MP at days 28 and 90, and by TAA at day 90. We have previously reported that a 28-day administration of TAA showed a similar pattern of increases in cell proliferation, and in cell populations immunoreactive to cell cycle-related molecules and apoptosis (Kimura *et al.*, 2015; Taniai *et al.*, 2012b; Yafune *et al.*, 2013b). Therefore, both TAA and MP have the potential to continuously facilitate cell proliferation and increase the number of p-Histone H3+, TOP2A+ and UBD+ cells, and apoptosis by repeated administration for more than 28 days. Considering the molecular function of UBD to facilitate the cell cycle by suppressing MAD2, a spindle checkpoint molecule (Herrmann *et al.*, 2007; Lim *et al.*, 2006), both TAA and MP continuously facilitate cell proliferation to cause an increase in cell cycle-arrested cells and apoptosis. In contrast, non-hepatocarcinogenic PMZ temporarily increased the number of Ki-67+, p-Histone H3+ and UBD+ cells at day 28, suggesting it is a false-positive compound among our candidates for early prediction markers of carcinogens. However, PMZ did not increase the number of cells immunoreactive to these molecules at day 90, suggesting that false-positive compounds may not continue cell cycle facilitation after long-term administration. It is difficult to detect carcinogen-specific responses by simple analysis of apoptosis and immunoreactive cell popu-

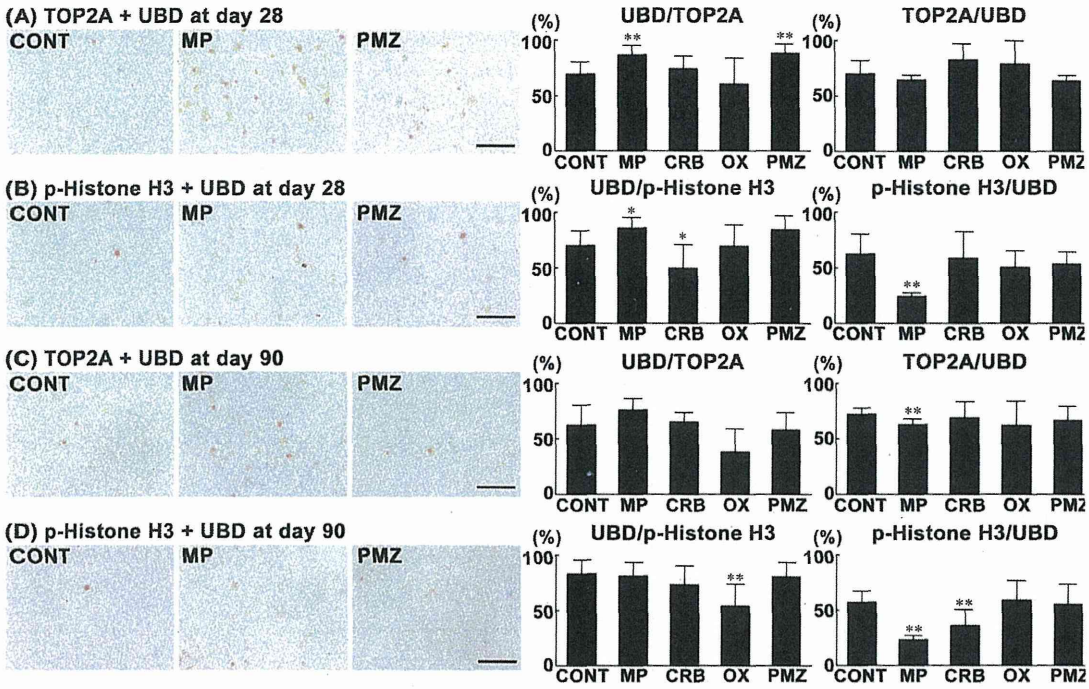

Fig. 5. Distribution of cell populations co-expressing TOP2A and UBD (UBD/TOP2A), UBD and TOP2A (TOP2A/UBD), p-Histone H3 and UBD (UBD/p-Histone H3), or UBD and p-Histone H3 (p-Histone H3/UBD) in the liver of rats at days 28 and 90. Photomicrographs show the distribution of TOP2A and UBD as well as p-Histone H3 and UBD in combination in the liver of representative cases from untreated controls and animals treated with MP or PMZ. The immunoreactivity of UBD (cytoplasm), and p-Histone H3 (nucleus) or TOP2A (nucleus) is visualized as brown and red, respectively. The graphs show the UBD-positive cell ratio (%) per total liver cells immunoreactive to TOP2A or p-Histone H3, and the TOP2A or p-Histone H3-positive cell ratio (%) per total liver cells immunoreactive to UBD counted in 10 animals of each group. Values represent mean + S.D. (A) UBD/TOP2A and TOP2A/UBD (day 28), (B) UBD/p-Histone H3 and p-Histone H3/UBD (day 28), (C) UBD/TOP2A and TOP2A/UBD (day 90), (D) UBD/p-Histone H3 and p-Histone H3/UBD (day 90). Bar = 100 μm. *, ** $P < 0.05$, 0.01, respectively, vs. untreated controls (Dunnett's or Steel's test).

lations to each molecule with our markers by day 28 of treatment. Importantly, CRB, LMG, BNF and OX did not increase the cell populations immunoreactive to cell cycle-related molecules or apoptosis even after a 90-day administration, despite their potential to exert carcinogenicity or carcinogenic promoting activity (King, 1976; Mitsumori *et al.*, 1997; NTP, 2005; Shoda *et al.*, 2000). These results suggest that hepatocarcinogens and hepatocarcinogenic promoters that do not facilitate cell proliferation after a 28-day administration do not facilitate cell proliferation, cell cycle and apoptosis even after a 90-day administration.

We have previously reported that hepatocarcinogens specifically upregulated *Mad2l1*, a spindle checkpoint gene (Weaver and Cleveland, 2005), and *Chek1*, a G_2/M checkpoint gene that responds to DNA damage (Patil *et al.*, 2013), after a 28-day administration, suggesting the presence of G_2 and M phase-arrested hepatocyte populations after hepatocarcinogen treatment (Kimura *et al.*, 2015). In the present study, hepatocarcinogenic MP increased the transcript levels of *Mad2l1* and *Chek1* at days 28 and 90, as previously reported (Kimura *et al.*, 2015). However, non-hepatocarcinogenic PMZ also increased the expression of these genes at day 28, while facilitating cell proliferation and cell cycle. We have also reported that chemicals facilitating cell proliferation increased cell populations immunoreactive to MAD2 and γH2AX, a DNA damage marker (Burma *et al.*, 2001), after a 28-day administration irrespective of their carcinogenic potential (Kimura *et al.*, 2015). It has been reported that several molecules that function in the G_2/M checkpoint, such as CHK1, also play essential roles in DNA replication, cell cycle control, development, meiosis and mitosis (O'Neil and Rose, 2006). These results suggest

Table 4. Relative transcript levels in the liver of rats treated with MP, CRB, OX or PMZ at day 28 and day 90.

Gene	Relative transcript level normalized to *Hprt1*				Relative transcript level normalized to *Actb*			
	MP[a]	CRB[a]	OX[a]	PMZ[a]	MP[a]	CRB[a]	OX[a]	PMZ[a]
Day 28								
Cdkn1a	0.77 ± 0.13	1.88 ± 0.36**	1.02 ± 0.23	0.25 ± 0.09**	1.05 ± 0.13	2.23 ± 0.55**	1.36 ± 0.42	0.29 ± 0.04**
Chek1	1.57 ± 0.36*	0.81 ± 0.28	1.34 ± 0.23	1.51 ± 0.05*	2.17 ± 0.51**	0.95 ± 0.34	1.73 ± 0.20**	2.11 ± 0.38**
Mad2l1	1.93 ± 0.49**	0.82 ± 0.13	0.79 ± 0.16*	1.18 ± 0.11*	2.64 ± 0.63**	0.95 ± 0.10	1.03 ± 0.19	1.70 ± 0.38**
Mdm2	1.80 ± 0.27**	1.89 ± 0.31**	1.39 ± 0.18**	1.03 ± 0.10	2.49 ± 0.36**	2.22 ± 0.44**	1.82 ± 0.33**	1.26 ± 0.31
Rbl2	0.45 ± 0.13**	1.06 ± 0.18	0.97 ± 0.17	0.88 ± 0.32	0.62 ± 0.20**	1.24 ± 0.20*	1.27 ± 0.28	1.01 ± 0.14
Tp53	1.38 ± 0.25*	1.04 ± 0.16	1.17 ± 0.20	1.21 ± 0.27	1.89 ± 0.24**	1.24 ± 0.28	1.53 ± 0.33**	1.52 ± 0.71
Day 90								
Cdkn1a	0.93 ± 0.21	2.58 ± 0.85**	0.76 ± 0.27	0.20 ± 0.05**	1.00 ± 0.43	2.60 ± 1.03**	0.81 ± 0.32	0.23 ± 0.03**
Chek1	2.05 ± 0.25**	0.94 ± 0.24	0.71 ± 0.09*	1.10 ± 0.20	2.13 ± 0.46*	0.94 ± 0.28	0.74 ± 0.08	1.25 ± 0.22
Mad2l1	3.03 ± 0.38**	0.99 ± 0.14	1.03 ± 0.22	0.96 ± 0.26	3.20 ± 0.87**	1.00 ± 0.23	1.07 ± 0.19	1.07 ± 0.14
Mdm2	1.69 ± 0.37**	1.99 ± 0.76*	1.18 ± 0.13	1.03 ± 0.22	1.70 ± 0.18**	2.07 ± 1.00	1.23 ± 0.21	1.19 ± 0.34
Rbl2	0.70 ± 0.16**	0.92 ± 0.07	1.04 ± 0.11	0.82 ± 0.15*	0.71 ± 0.13**	0.92 ± 0.12	1.08 ± 0.12	0.93 ± 0.13
Tp53	1.49 ± 0.23**	0.93 ± 0.25	0.76 ± 0.14*	1.03 ± 0.13	1.55 ± 0.42	0.91 ± 0.12	0.79 ± 0.11	1.19 ± 0. 30

Abbreviations: *Actb*, actin, beta; *Cdkn1a*, cyclin-dependent kinase inhibitor 1A; *Chek1*, checkpoint kinase 1; CRB, carbadox; *Hprt1*, hypoxanthine phosphoribosyltransferase 1; *Mad2l1*, MAD2 mitotic arrest deficient-like 1 (yeast); *Mdm2*, MDM2 proto-oncogene, E3 ubiquitin protein ligase; MP, methapyrilene; OX, oxfendazole; PMZ, promethazine; *Rbl2*, retinoblastoma-like 2; *Tp53*, tumor protein p53. [a] n = 6. Values represent relative expression levels expressed as mean ± S.D. * $P < 0.05$, ** $P < 0.01$ vs. untreated controls (Dunnett's or Steel's test).

that upregulation of *Mad2l1* and *Chek1* after a 28-day administration with chemicals facilitating cell proliferation may reflect the activation of G_2/M and spindle checkpoint functions simply in association with cell proliferation activity.

$p21^{Cip1}$ is one of the cyclin-dependent kinase inhibitors that lead to cell cycle arrest at G_1 phase and its expression is usually regulated by p53 (Abbas and Dutta, 2009). We have previously reported that hepatocarcinogens specifically increase the number of $p21^{Cip1+}$ cells, reflecting activation of G_1/S checkpoint, after a 28-day administration in rats, hence it was expected to be an early prediction marker of carcinogens in several target organs, such as the liver, thyroid, urinary bladder and glandular stomach (Yafune *et al.*, 2013a, 2013b). However, in the present study, hepatocarcinogenic MP did not increase the number of $p21^{Cip1+}$ cells at days 28 and 90. On the other hand, non-hepatocarcinogenic APAP and PMZ increased $p21^{Cip1+}$ cells at day 90. It has been reported that expression of $p21^{Cip1}$ is induced by a variety of stimuli, such as DNA damage, oxidative stress, cytokine action and metabolic deficiencies (Abbas and Dutta, 2009; Gorospe *et al.*, 1999). It has also been reported that treatment with APAP induced oxidative stress in the acute stage of an administration study in rat liver (El-Shafey *et al.*, 2015). However, there are no studies that examined oxidative stress responses after subchronic administration in rodents. PMZ has been shown to be a powerful inhibitor of iron-dependent liposomal lipid peroxidation, scavenger of organic peroxyl radicals and inhibitor of heme protein/hydrogen peroxide-dependent peroxidation of arachidonic acid (Jeding *et al.*, 1995). In the present study, we found decreased expression of *Cdkn1a*, encoding $p21^{Cip1}$, at 28 and 90 days of PMZ treatment, in contrast to the increase in the number of $p21^{Cip1+}$ cells at day 90. While the reason for this discrepancy between transcript expression and immunoreactive cell population is not clear, the transcript downregulation of *Cdkn1a* may be the reflection of antioxidant property of this compound. It has been reported that PMZ slows down protein degradation in rat liver (Fernández *et al.*, 1981). Therefore, PMZ may affect gene control by multiple mechanisms. While the mechanism of the increase in the number of $p21^{Cip1+}$ cells by APAP and PMZ at day 90 is not clear, an increase in the number of $p21^{Cip1+}$ cells may not always be a hepatocarcinogen-specific response.

We have previously reported that hepatocarcinogens facilitating cell proliferation specifically downregulat-

ed *Rbl2*, a gene encoding an RB family protein that regulates the progression of G_1/S phase (Cobrinik *et al.*, 1996; Cobrinik, 2005), after a 28-day administration (Kimura *et al.*, 2015). In the present study, similar results were found with hepatocarcinogenic MP at days 28 and 90. However, hepatocarcinogenic CRB did not change the transcript level of *Rbl2* in the present study at these time points. This compound also did not facilitate cell proliferation and apoptosis, and there were no fluctuations in cell populations immunoreactive to cell cycle-related molecules even after a 90-day administration, suggesting a linkage between *Rbl2* downregulation and carcinogens facilitating cell proliferation. However, non-hepatocarcinogenic PMZ also downregulated *Rbl2* at day 90, though at this stage PMZ no longer facilitated cell proliferation. These results suggest that downregulation of *Rbl2* may not be a hepatocarcinogen-specific response and may be unrelated to cell proliferation facilitation.

Here, hepatocarcinogens MP and CRB upregulated *Mdm2*, a p53 downstream molecule that facilitates degradation of both p53 and RB protein through facilitation of ubiquitination (Bhattacharya and Ghosh, 2014; Honda *et al.*, 1997; Uchida *et al.*, 2005), at days 28 and 90. CRB is classified as a genotoxic hepatocarcinogen (Beutin *et al.*, 1981; King, 1976). With regard to MP, there are some reports suggesting that MP has a potential to induce DNA damage in mouse lymphoma cells or rat hepatocytes, while other reports concluded that MP does not have genotoxic potential (NTP, 2000; Priestley *et al.*, 2011). We have previously reported that hepatocarcinogens specifically upregulated *Mdm2* and increased the number of p-MDM2$^+$ liver cells after a 28-day administration, suggesting facilitation of proteasome-mediated degradation of p53 and RB protein (Kimura *et al.*, 2015). In the present study, MP caused upregulation of *Tp53* and *Mdm2* from day 28 after starting administration. It is well known that p53 expression is induced in response to DNA damage (Gotz and Montenarh, 1995). Therefore, in the present study, MP may have upregulated MDM2 in association with p53 upregulation. However, CRB did not upregulate *Tp53*, while *Mdm2* upregulation was observed from day 28 after starting administration. It has been reported that MDM2 expression can also be regulated by p53-independent mechanisms, such as through activation of RAS, estrogen receptor-α and MYCN (Zhao *et al.*, 2014). Therefore, CRB may cause *Mdm2* upregulation via a p53-independent mechanism.

MDM2 phosphorylated at Ser 166, an activated isoform of MDM2, can translocate from the cytoplasm to the nucleus and facilitate degradation of p53 (Malmlöf *et al.*, 2007; Mayo and Donner, 2002). Here, MP at day 28 and TAA at day 90 increased the number of nuclear p-MDM2$^+$ cells accompanied with increased cell proliferation. LMG also increased the number of p-MDM2$^+$ cells at days 28 and 90, even though its potential to exert carcinogenicity is marginal (NTP, 2005). However, hepatocarcinogenic CRB at days 28 and 90, and MP at day 90 did not increase the number of p-MDM2$^+$ cells, while these hepatocarcinogens upregulated *Mdm2* expression at these time points. CRB did not facilitate apoptosis at both days 28 and 90, therefore, DNA damage may not have accumulated sufficiently to induce transcriptional activation of *Tp53* even after 90 days of administration in the present study. These results suggest that induction of MDM2 activation did not occur by CRB administration, while the transcript levels were upregulated at days 28 and 90. On the other hand, it has been reported that DNA damage can trigger MDM2 destruction (Inuzuka *et al.*, 2010). Therefore, no change in the number of p-MDM2$^+$ cells irrespective of *Tp53* upregulation after administration of MP for 90 days may be due to facilitation of MDM2 degradation in response to DNA damage. In contrast, non-carcinogenic hepatotoxicants and hepatocarcinogenic promoters caused neither upregulation of *Mdm2* expression nor increase in the number of p-MDM2$^+$ cells at days 28 and 90, while non-hepatocarcinogenic PMZ increased cell proliferation at day 28. These results suggest that hepatocarcinogens may induce *Mdm2* upregulation or increase the number of p-MDM2$^+$ cells from day 28 after starting administration, reflecting facilitation of p53 and Rb protein degradation. Considering CRB and LMG caused *Mdm2* upregulation or increase in the number of p-MDM2$^+$ cells without facilitating cell proliferation, MDM2 activation may not directly induce cell cycle facilitation.

It has been reported that overexpression of UBD suppressed the kinetochore localization of MAD2, a spindle checkpoint molecule, during M phase, which may eventually lead to chromosomal instability (Herrmann *et al.*, 2007; Lim *et al.*, 2006). We have previously reported that a 28-day administration of carcinogens facilitating cell proliferation caused aberrant expression of UBD at G_2 phase, suggestive of disruption of spindle checkpoint function (Kimura *et al.*, 2015; Taniai *et al.*, 2012b). In the present study, MP, facilitating cell proliferation from day 28 after starting administration, decreased the number of p-Histone H3$^+$ cells within the UBD$^+$ cell population at days 28 and 90. On the other hand, CRB also decreased the number of p-Histone H3$^+$ cells within the UBD$^+$ cell population at day 90, while CRB did not induce cell proliferation even after a 90-day administration. In contrast, hepatocarcinogenic promoter OX or non-hepatocarcinogenic PMZ did not cause these changes even

after 90 days of administration. Because p-Histone H3 is expressed at M phase (Hirota *et al.*, 2005), these results suggest that hepatocarcinogens may specifically reduce UBD expression at M phase, irrespective of their ability to increase cell proliferation. Furthermore, MP decreased the p-Histone $H3^+$/Ki-67^+ cell ratio at days 28 and 90, as did CRB at day 90, suggesting an increase in proliferating cells accelerating M phase transition probably because of spindle checkpoint disruption. It has been reported that the UBD-MAD2 interaction reduces the proportion of cells at M phase within the proliferating cell population and induces abnormalities in chromosome structure and number, reflecting spindle checkpoint disruption (Theng *et al.*, 2014). Therefore, hepatocarcinogens may specifically induce disruption of spindle checkpoint function and subsequent chromosomal instability, leading to carcinogenesis, while this change may not always induce an increase in cell proliferation. In contrast, carcinogen-specific responses were not observed in the number of UBD^+ cells within the $TOP2A^+$ cell population or the number of UBD^+ cells within the p-Histone $H3^+$ cell population in the present study. These results suggest that among the parameters examined in the present study, the decrease in the number of p-Histone $H3^+$ cells within the UBD^+ cell population is the most reliable parameter for prediction of the carcinogenic potential of chemicals.

In conclusion, hepatocarcinogens facilitating cell proliferation at day 28 continuously facilitated cell proliferation, cell cycle and apoptosis for up to 90 days. In immunohistochemical single molecule analysis, hepatocarcinogen- or hepatocarcinogenic promoter-specific cellular responses were not observed even after 90 days of administration. Hepatocarcinogen- or hepatocarcinogenic promoter-specific cellular responses were also not observed in the transcript levels of *Cdkn1a*, *Mad2l1*, *Chek1* and *Rbl2*. On the other hand, all hepatocarcinogens and LMG induced *Mdm2* upregulation or an increase in the number of p-$MDM2^+$ cells from day 28, irrespective of the lack of facilitation of cell proliferation activity by some compounds. However, different *Tp53* expression levels suggest different mechanisms of induction or activation of MDM2 among hepatocarcinogens. On the other hand, hepatocarcinogenic MP and CRB induced a decrease in both UBD^+ cells and proliferating cells remaining in M phase at day 28 and/or day 90, irrespective of the lack of facilitation of cell proliferation by the latter. These results suggest that hepatocarcinogens specifically induce disruption of spindle checkpoint function after 28 or 90 days of administration, which may be induced ahead of facilitation of cell proliferation.

ACKNOWLEDGMENTS

The authors thank Mrs. Shigeko Suzuki for her technical assistance in preparing the histological specimens. This work was supported by Health and Labour Sciences Research Grants (Research on Food Safety) from the Ministry of Health, Labour and Welfare of Japan (Grant No. H25-shokuhin-ippan-005). All authors disclose that there are no conflicts of interest that could inappropriately influence the outcome of the present study. M.K. is a Research Fellow of the Japan Society for the Promotion of Science.

Conflict of interest---- The authors declare that there is no conflict of interest.

REFERENCES

Abbas, T. and Dutta, A. (2009): p21 in cancer: intricate networks and multiple activities. Nat. Rev. Cancer, **9**, 400-414.

Becker, F.F. (1983): Thioacetamide hepatocarcinogenesis. J. Natl. Cancer Inst., **71**, 553-558.

Beutin, L., Preller, E. and Kowalski, B. (1981): Mutagenicity of quindoxin, its metabolites, and two substituted quinoxaline-di-N-oxides. Antimicrob. Agents Chemother., **20**, 336-343.

Bhattacharya, S. and Ghosh, M.K. (2014): HAUSP, a novel deubiquitinase for Rb - MDM2 the critical regulator. FEBS J., **281**, 3061-3078.

Burma, S., Chen, B.P., Murphy, M., Kurimasa, A. and Chen, D.J. (2001): ATM phosphorylates histone H2AX in response to DNA double-strand breaks. J. Biol. Chem., **276**, 42462-42467.

Cobrinik, D., Lee, M.H., Hannon, G., Mulligan, G., Bronson, R.T., Dyson, N., Harlow, E., Beach, D., Weinberg, R.A. and Jacks, T. (1996): Shared role of the pRB-related p130 and p107 proteins in limb development. Genes Dev., **10**, 1633-1644.

Cobrinik, D. (2005): Pocket proteins and cell cycle control. Oncogene, **24**, 2796-2809.

Eastin, W.C. (1998): The U.S. National toxicology program evaluation of transgenic mice as predictive models for identifying carcinogens. Environ. Health Perspect., **106**, 81-84.

Eckle, V.S., Buchmann, A., Bursch, W., Schulte-Hermann, R. and Schwarz, M. (2004): Immunohistochemical detection of activated caspases in apoptotic hepatocytes in rat liver. Toxicol. Pathol., **32**, 9-15.

El-Shafey, M.M., Abd-Allah, G.M., Mohamadin, A.M., Harisa, G.I. and Mariee, A.D. (2015): Quercetin protects against acetaminophen-induced hepatorenal toxicity by reducing reactive oxygen and nitrogen species. Pathophysiology, **22**, 49-55.

Fernández, G., Villarruel, M.C., Bernacchi, A., de Castro, C.R. and Castro, J.A. (1981): Liver microsomal drug-metabolizing enzyme activity: enhancement by blockade of degradative processes in promethazine-treated rats. Br. J. Exp. Pathol., **62**, 440-445.

Gorospe, M., Wang, X. and Holbrook, N.J. (1999): Functional role of p21 during the cellular response to stress. Gene Expr., **7**, 377-385.

Gotz, C. and Montenarh, M. (1995): P53 and its implication in apoptosis (review). Int. J. Oncol., **6**, 1129-1135.

Hayashi, H., Taniai, E., Morita, R., Hayashi, M., Nakamura, D., Wakita, A., Suzuki, K., Shibutani, M. and Mitsumori, K. (2012): Enhanced liver tumor promotion but not liver initiation activity in rats subjected to combined administration of omeprazole and β-naphthoflavone. J. Toxicol. Sci., **37**, 969-985.

Herrmann, J., Lerman, L.O. and Lerman, A. (2007): Ubiquitin and ubiquitin-like proteins in protein regulation. Circ. Res., **100**, 1276-1291.

Hirota, T., Lipp, J.J., Toh, B.H. and Peters, J.M. (2005): Histone H3 serine 10 phosphorylation by Aurora B causes HP1 dissociation from heterochromatin. Nature, **438**, 1176-1180.

Honda, R., Tanaka, H. and Yasuda, H. (1997): Oncoprotein MDM2 is a ubiquitin ligase E3 for tumor suppressor p53. FEBS Lett., **420**, 25-27.

Inuzuka, H., Tseng, A., Gao, D., Zhai, B., Zhang, Q., Shaik, S., Wan, L., Ang, X.L., Mock, C., Yin, H., Stommel, J.M., Gygi, S., Lahav, G., Asara, J., Xiao, Z.X., Kaelin, W.G.Jr., Harper, J.W. and Wei, W. (2010): Phosphorylation by casein kinase I promotes the turnover of the Mdm2 oncoprotein via the SCF(beta-TRCP) ubiquitin ligase. Cancer Cell, **18**, 147-159.

Jeding, I., Evans, P.J., Akanmu, D., Dexter, D., Spencer, J.D., Aruoma, O.I., Jenner, P. and Halliwell, B. (1995): Characterization of the potential antioxidant and pro-oxidant actions of some neuroleptic drugs. Biochem. Pharmacol., **49**, 359-365.

Jonker, M.J., Bruning, O., van Iterson, M., Schaap, M.M., van der Hoeven, T.V., Vrieling, H., Beems, R.B., de Vries, A., van Steeg, H., Breit, T.M. and Luijten, M. (2009): Finding transcriptomics biomarkers for *in vivo* identification of (non-)genotoxic carcinogens using wild-type and Xpa/p53 mutant mouse models. Carcinogenesis, **30**, 1805-1812.

Kimura, M., Abe, H., Mizukami, S., Tanaka, T., Itahashi, M., Onda, N., Yoshida, T. and Shibutani, M. (2015): Onset of hepatocarcinogen-specific cell proliferation and cell cycle aberration during the early stage of repeated hepatocarcinogen administration in rats. J. Appl. Toxicol., doi: 10.1002/jat.3163.

King, T.O. (1976): Target Organ Toxicity of GS-6244 (carbadox) and CP-17,056 (desoxycarbadox) with Chronic Administration in Rats. Unpublished. Submitted to WHO by Pfizer Central Research, Groton, CT, USA.

Lim, C.B., Zhang, D. and Lee, C.G. (2006): FAT10, a gene up-regulated in various cancers, is cell-cycle regulated. Cell Div., **1**, 20.

Livak, K.J. and Schmittgen, T.D. (2001): Analysis of relative gene expression data using real-time quantitative PCR and the $2^{-\Delta\Delta C_T}$ method. Methods, **25**, 402-408.

Malmlöf, M., Roudier, E., Högberg, J. and Stenius, U. (2007): MEK-ERK-mediated phosphorylation of Mdm2 at Ser-166 in hepatocytes. Mdm2 is activated in response to inhibited Akt signaling. J. Biol. Chem., **282**, 2288-2296.

Mattila, R., Alanen, K. and Syrjänen, S. (2007): Immunohistochemical study on topoisomerase IIα, Ki-67 and cytokeratin-19 in oral lichen planus lesions. Arch. Dermatol. Res., **298**, 381-388.

Mayo, L.D. and Donner, D.B. (2002): The PTEN, Mdm2, p53 tumor suppressor-oncoprotein network. Trends Biochem. Sci., **27**, 462-467.

McKillop, D. and Case, D.E. (1991): Mutagenicity, carcinogenicity and toxicity of beta-naphthoflavone, a potent inducer of P448. Biochem. Pharmacol., **41**, 1-7.

Mitsumori, K., Onodera, H., Shoda, T., Uneyama, C., Imazawa, T., Takegawa, K., Yasuhara, K., Watanabe, T. and Takahashi, M. (1997): Liver tumour-promoting effects of oxfendazole in rats. Food Chem. Toxicol., **35**, 799-806.

NTP (1993a): NTP Toxicology and Carcinogenesis Studies of Acetaminophen (CAS No. 103-90-2) in F344 Rats and B6C3F1 Mice (Feed Studies). Natl. Toxicol. Program Tech. Rep. Ser., **394**, 1-274.

NTP (1993b): NTP Toxicology and Carcinogenesis Studies of Promethazine Hydrochloride (CAS No. 58-33-3) in F344/N Rats and B6C3F1 Mice (Gavage Studies). Natl. Toxicol. Program Tech. Rep. Ser., **425**, 1-272.

NTP (2000): NTP Hepatotoxicity Studies of the Liver Carcinogen Methapyrilene Hydrochloride (CAS No. 135-23-9) Administered in Feed to Male F344/N Rats. Toxic. Rep. Ser., **46**, 1-C7.

NTP (2005): Toxicology and carcinogenesis studies of malachite green chloride and leucomalachite green. (CAS NOS. 569-64-2 and 129-73-7) in F344/N rats and B6C3F1 mice (feed studies). Natl. Toxicol. Program. Tech. Rep. Ser., **527**, 1-312.

O'Neil, N. and Rose, A. (2006): DNA repair. WormBook, **13**, 1-12.

Patil, M., Pabla, N. and Dong, Z. (2013): Checkpoint kinase 1 in DNA damage response and cell cycle regulation. Cell. Mol. Life Sci., **70**, 4009-4021.

Scholzen, T. and Gerdes, J. (2000): The Ki-67 protein: from the known and the unknown. J. Cell. Physiol., **182**, 311-322.

Sherr, C.J. and Roberts, J.M. (1995): Inhibitors of mammalian G1 cyclin-dependent kinases. Genes. Dev., **9**, 1149-1163.

Shoda, T., Mitsumori, K., Onodera, H., Toyoda, K., Uneyama, C., Takada, K. and Hirose, M. (2000): Liver tumor-promoting effect of beta-naphthoflavone, a strong CYP 1A1/2 inducer, and the relationship between CYP 1A1/2 induction and Cx32 decrease in its hepatocarcinogenesis in the rat. Toxicol. Pathol., **28**, 540-547.

Tamano, S. (2010): Carcinogenesis risk assessment of chemicals using medium-term carcinogenesis bioassays. Asian Pac. J. Cancer Prev., **11**, 4-5.

Taniai, E., Hayashi, H., Yafune, A., Watanabe, M., Akane, H., Suzuki, K., Mitsumori, K. and Shibutani, M. (2012a): Cellular distribution of cell cycle-related molecules in the renal tubules of rats treated with renal carcinogens for 28 days: relationship between cell cycle aberration and carcinogenesis. Arch. Toxicol., **86**, 1453-1464.

Taniai, E., Yafune, A., Hayashi, H., Itahashi, M., Hara-Kudo, Y., Suzuki, K., Mitsumori, K. and Shibutani, M. (2012b): Aberrant activation of ubiquitin D at G_2 phase and apoptosis by carcinogens that evoke cell proliferation after 28-day administration in rats. J. Toxicol. Sci., **37**, 1093-1111.

Theng, S.S., Wang, W., Mah, W.C., Chan, C., Zhuo, J., Gao, Y., Qin, H., Lim, L., Chong, S.S., Song, J. and Lee, C.G. (2014): Disruption of FAT10-MAD2 binding inhibits tumor progression. Proc. Natl. Acad. Sci. USA, **111**, E5282-5291.

Uchida, C., Miwa, S., Kitagawa, K., Hattori, T., Isobe, T., Otani, S., Oda, T., Sugimura, H., Kamijo, T., Ookawa, K., Yasuda, H. and Kitagawa, M. (2005): Enhanced Mdm2 activity inhibits pRB function via ubiquitin-dependent degradation. EMBO J., **24**, 160-169.

Uehara, T., Minowa, Y., Morikawa, Y., Kondo, C., Maruyama, T., Kato, I., Nakatsu, N., Igarashi, Y., Ono, A., Hayashi, H., Mitsumori, K., Yamada, H., Ohno, Y. and Urushidani, T. (2011): Prediction model of potential hepatocarcinogenicity of rat hepatocarcinogens using a large-scale toxicogenomics database. Toxicol. Appl. Pharmacol., **255**, 297-306.

Weaver, B.A. and Cleveland, D.W. (2005): Decoding the links between mitosis, cancer, and chemotherapy: The mitotic checkpoint, adaptation, and cell death. Cancer Cell, **8**, 7-12.

WHO (1991): Evaluation of certain veterinary drug residues in food. Thirty-eighth report of the Joint FAO/WHO Expert Com-

mittee on Food Additives. World Health Organ Tech. Rep. Ser., **815**, 1-64.

Yafune, A., Taniai, E., Morita, R., Nakane, F., Suzuki, K., Mitsumori, K. and Shibutani, M. (2013a): Expression patterns of cell cycle proteins in the livers of rats treated with hepatocarcinogens for 28 days. Arch. Toxicol., **87**, 1141-1153.

Yafune, A., Taniai, E., Morita, R., Hayashi, H., Suzuki, K., Mitsumori, K. and Shibutani, M. (2013b): Aberrant activation of M phase proteins by cell proliferation-evoking carcinogens after 28-day administration in rats. Toxicol. Lett., **219**, 203-210.

Zhao, Y., Yu, H. and Hu, W. (2014): The regulation of MDM2 oncogene and its impact on human cancers. Acta. Biochim. Biophys. Sin. (Shanghai), **46**, 180-189.

The Journal of Toxicological Sciences (J. Toxicol. Sci.)
Vol.41, No.1, 91-104, 2016

Original Article

Disruption of spindle checkpoint function in rats following 28 days of repeated administration of renal carcinogens

Masayuki Kimura[1,2], Sayaka Mizukami[1,2], Yousuke Watanabe[1,2], Yasuko Hasegawa-Baba[1], Nobuhiko Onda[1], Toshinori Yoshida[1] and Makoto Shibutani[1]

[1]*Laboratory of Veterinary Pathology, Tokyo University of Agriculture and Technology, 3-5-8 Saiwai-cho, Fuchu-shi, Tokyo 183-8509, Japan*
[2]*Pathogenetic Veterinary Science, United Graduate School of Veterinary Sciences, Gifu University, 1-1 Yanagido, Gifu-shi, Gifu 501-1193, Japan*

(Received September 19, 2015; Accepted November 4, 2015)

ABSTRACT — We previously reported that 28-day exposure to hepatocarcinogens that facilitate cell proliferation specifically alters the expression of G_1/S checkpoint-related genes and proteins, induces aberrant early expression of ubiquitin D (UBD) at the G_2 phase, and increases apoptosis in the rat liver, indicating G_1/S and spindle checkpoint dysfunction. The present study aimed to determine the time of onset of carcinogen-specific cell-cycle disruption after repeated administration of renal carcinogens for up to 28 days. Rats were orally administered the renal carcinogens nitrofurantoin (NFT), 1-amino-2,4-dibromoantraquinone (ADAQ), and 1,2,3-trichloropropane (TCP) or the non-carcinogenic renal toxicants 1-chloro-2-propanol, triamterene, and carboxin for 3, 7 or 28 days. Both immunohistochemical single-molecule analysis and real-time RT-PCR analysis revealed that carcinogen-specific expression changes were not observed after 28 days of administration. However, the renal carcinogens ADAQ and TCP specifically reduced the number of cells expressing phosphorylated-histone H3 at Ser10 in both UBD^+ cells and proliferating cells, suggestive of insufficient UBD expression at the M phase and early transition of proliferating cells from the M phase, without increasing apoptosis, after 28 days of administration. In contrast, NFT, which has marginal carcinogenic potential, did not induce such cellular responses. These results suggest that it may take 28 days to induce spindle checkpoint dysfunction by renal carcinogens; however, induction of apoptosis may not be essential. Thus, induction of spindle checkpoint dysfunction may be dependent on carcinogenic potential of carcinogen examined, and marginal carcinogens may not exert sufficient responses even after 28 days of administration.

Key words: Cell proliferation, Renal carcinogen, Spindle checkpoint, Ubiquitin D, Apoptosis

INTRODUCTION

One of the most reliable methods to evaluate the carcinogenicity of chemicals involves exposing rodent animals to test compounds for 1.5 or 2 years. However, these bioassays are time consuming and expensive, and involve the use of hundreds of animals. To resolve these problems, alternative methods have been developed, such as the two-stage carcinogenesis model (Tamano, 2010) and genetically modified animals produced by transgenic or gene targeting technologies (Eastin, 1998). However, these methods are also laborious and expensive, and have limited target organs. Although toxicogenomic approaches for the prediction of carcinogenic potential in each target organ may be promising (Jonker *et al.*, 2009; Matsumoto *et al.*, 2014), these methods also require integrative methodologies between different laboratories sharing expression databases. Therefore, the development of rapid and inexpensive assays for evaluating or predicting the carcinogenic potential of chemicals based on the molecular responses to the carcinogens in the target organs would be advantageous.

We have previously analyzed cell-cycle proteins in a study of 28-day repeated treatment with carcinogens. We found that carcinogens facilitating cell proliferation in carcinogenic target cells also induced aberrant expression of cell-cycle proteins involved in the activation of G_1/S and G_2/M checkpoint functions to cause cell-cycle

Correspondence: Makoto Shibutani (E-mail: mshibuta@cc.tuat.ac.jp)

arrest and apoptosis irrespective of the target organ after a 28-day administration period (Taniai *et al.*, 2012a, 2012b; Yafune *et al.*, 2013a, 2013b). In addition, we found that such carcinogens typically induced an aberrant shift in the expression of ubiquitin D (UBD), a spindle checkpoint inhibitor (Herrmann *et al.*, 2007; Lim *et al.*, 2006), at the G_2 phase in carcinogenic target cells, indicating spindle checkpoint dysfunction at the M phase (Taniai *et al.*, 2012b; Kimura *et al.*, 2015a). These results suggest that carcinogens facilitating cell proliferation in target cells induce aberrant cell-cycle control, including disruption of spindle checkpoint function, which may be a common cellular response to carcinogens. Furthermore, we have also recently found that some hepatocarcinogens specifically caused the downregulation of *Rbl2*, upregulation of *Mdm2*, and increase the number of phosphorylated-E3 ubiquitin-protein ligase MDM2 $(p\text{-}MDM2)^+$ cells, suggestive of disruption to G_1/S checkpoint function, as well as spindle checkpoint dysfunction, only after 28 days of administration (Kimura *et al.*, 2015a). Moreover, in a study of repeated administration of hepatocarcinogens for up to 90 days, hepatocarcinogen carbadox caused disruption of spindle checkpoint function after 90 days of administration, while this compound did not facilitate cell proliferation at this time point (Kimura *et al.*, 2015b). These results suggest that carcinogen-specific disruption of spindle checkpoint function may be induced after 28 or 90 days of administration of hepatocarcinogens, which may be induced ahead of facilitation of cell proliferation at initial stage of carcinogenesis. However, it is not clear whether the time of onset of aberrant cell-cycle regulation specifically observed with hepatocarcinogens could be applied to carcinogens targeting other organs.

The present study aimed to determine the time of onset of carcinogen-specific disruption of cell-cycle regulation during a time course of repeated administration of renal carcinogens. For this purpose, rats were repeatedly administered renal carcinogens or non-carcinogenic renal toxicants for up to 28 days, and the time course response in cell proliferation activity, expression of G_1/S, G_2/M, and spindle checkpoint-related molecules, and apoptosis were examined using immunohistochemistry and/or real-time reverse transcription polymerase chain reaction (RT-PCR).

MATERIALS AND METHODS

Chemicals

Nitrofurantoin (NFT; CAS No. 67-20-9, purity > 98.0%) and triamterene (TAT; CAS No. 396-01-0, purity > 98.0%) were purchased from Tokyo Chemical Industry Co. Ltd. (Tokyo, Japan). 1-Amino-2,4-dibromoantraquinone (ADAQ; CAS No. 81-49-2, purity ≥ 97%), carboxin (CBX; CAS No. 5234-68-4, purity ≥ 95%), 1-chloro-2-propanol (CP; CAS No. 127-00-4, purity 75% to 76% 1-chloro-2-propanol; 24% to 25% 2-chloro-1-propanol), 1,2,3-trichloropropane (TCP; CAS No. 96-18-4, purity ≥ 99%) were purchased from Wako Pure Chemicals Industries (Osaka, Japan). Corn oil was purchased from Hayashi Chemicals Co. Ltd. (Tokyo, Japan).

Animal experiments

Five-week-old male F344/NSlc rats were purchased from Japan SLC, Inc. (Shizuoka, Japan), and acclimatized to a powdered basal diet (CRF-1; Oriental Yeast Co., Tokyo, Japan) and tap water *ad libitum* for one week. Rats were housed in plastic cages with paper chip in a barrier-maintained animal room under standard conditions (room temperature, 23 ± 3°C; relative humidity, 50 ± 20%; 12-hr light/dark cycle).

In the present study, animals were administered renal carcinogens (NFT, ADAQ, or TCP) or non-carcinogenic renal toxicants (CP, TAT, or CBX). Animals were repeatedly administered test chemicals for 3, 7 and 28 days. After administration, cell proliferation activity, expression of cell cycle-related molecules, and apoptosis were examined using immunohistochemistry and/or real-time RT-PCR.

NFT, ADAQ, and TCP were selected as renal carcinogens (National Toxicology Program [NTP], 1989; NTP, 1993a; NTP, 1996) and CP, TAT, and CBX were selected as non-carcinogenic renal toxicants (NTP, 1993b; NTP, 1998; US Environmental Protection Agency [USEPA], 2004).

Animals were divided into seven groups based on initial body weights and administered NFT in basal diet (n = 33), ADAQ (25,000 ppm) in basal diet (n = 33), TCP (125 mg/kg body weight) daily by gavage in corn oil (n = 33), CP (3,300 ppm) in drinking water (n = 30), TAT (1,200 ppm) in basal diet (n = 30) or CBX (2,000 ppm) in basal diet (n = 30) for 3, 7 or 28 days. In the NFT group, the initial dose was set at 5,000 ppm in the diet. However, as the general condition of the animals worsened, the dose was reduced to 4,000 ppm after 9 days from starting administration and 3,000 ppm after 14 days. Untreated controls (n = 30) were maintained on the basal diet and tap water without any treatment during the experimental period. After the 3, 7 or 28 days of treatment, one third (n = 10 or 11) of the animals in each group were euthanized by exsanguination from the abdominal aorta under deep anesthesia with CO_2/O_2 and kidneys were removed.

The dose levels of NFT, ADAQ, and TCP, even after

the dose change in case of NFT, have been shown to induce kidney tumors in rats (NTP, 1989; NTP, 1993a; NTP, 1996). The dose levels of CP, TAT, and CBX induced nephrotoxicity after a 13- or 14-week administration in rats (NTP, 1993b; NTP, 1998; USEPA, 2004).

All animal experiments were conducted in accordance with the "Guidelines for Proper Conduct of Animal Experiments" (Science Council of Japan, June 1, 2006), and the animal protocols were reviewed and approved by the Animal Care and Use Committee of the Tokyo University of Agriculture and Technology. All efforts were made to minimize animal suffering.

Histology and immunohistochemistry

Three-micrometer sections of paraffin-embedded tissues from the kidney were stained with hematoxylin and eosin for histopathological examination, or subjected to immunohistochemistry. Immunohistochemistry of kidney sections was performed using the Vectastain® Elite ABC Kit (Vector Laboratories Inc., Burlingame, CA, USA) with 3,3'-diaminobenzidine/H_2O_2 as the chromogen and the following antibodies: Ki-67, a marker of cell proliferation expressing in the nucleus during the G_1 to M phase of the cell cycle (Scholzen and Gerdes, 2000), phosphorylated histone H3 (p-Histone H3), acting on chromosome condensation at the early M phase (Hirota *et al.*, 2005), topoisomerase II alpha (TOP2A), acting on DNA decatenation at G_2/M phase (Mattila *et al.*, 2007), UBD, a molecule that leads to chromosomal instability through reduction in kinetochore localization of checkpoint proteins, such as mitotic arrest deficient-2 (MAD2), during the G_2/M phase (Herrmann *et al.*, 2007; Lim *et al.*, 2006), and p-MDM2 (Ser 166), a p53 downstream molecule that facilitates degradation of p53 (Malmlöf *et al.*, 2007; Mayo and Donner, 2002). Antigen retrieval conditions and the concentrations of each antibody are shown in Supplementary Table 1. Immunostained sections were counterstained with hematoxylin for microscope examination. Endogenous peroxidase activity was blocked with 0.3% hydrogen peroxide.

For evaluation of apoptosis, the terminal deoxynucleotidyl transferase dUTP nick end labeling (TUNEL) assay was performed using the ApopTag *In Situ* Apoptosis Detection Kit (Millipore Corporation, Billerica, MA, USA) according to the manufacturer's protocol. Briefly, deparaffinized sections were treated with 20 μg/mL proteinase K for 15 min at room temperature. Endogenous peroxidase activity was blocked with 3.0% hydrogen peroxide. Color development and counter staining were as described above for immunohistochemistry.

To estimate the ratio of UBD^+ cells colocalized with TOP2A or p-Histone H3 to the total number of UBD^+ cells, double immunohistochemistry of UBD with TOP2A or p-Histone H3 was conducted. For this purpose, the Vectastain® Elite ABC Kit (Vector Laboratories Inc.) with 3,3'-diaminobenzidine was used to visualize UBD and the Vectastain® ABC-AP kit (Vector Laboratories Inc.) with Vector Red Alkaline Phosphate Substrate Kit I (Vector Laboratories Inc.) was used to visualize TOP2A and p-Histone H3.

Analysis of immunoreactivity

In our previous study, all tested renal carcinogens increased cells expressing cell cycle proteins as candidate prediction markers of carcinogenicity in analysis of the outer stripe of the outer medulla (OSOM), while *p*-nitrobenzoic acid, a non-carcinogenic renal toxicant, also increased cells expressing cell cycle proteins in analysis of the whole cortical area and OSOM (Taniai *et al.*, 2012a, 2012b). Therefore, only OSOM areas were selected for analysis of immunoreactive cells to avoid detecting false-positive responses in the present study.

The immunoreactive cells for Ki-67, p-Histone H3, TOP2A, UBD, and p-MDM2 and $TUNEL^+$ apoptotic cells were counted in 10 randomly selected areas per animal (5 areas per kidney) at 400 × magnification, avoiding areas of connective tissues and vasculature. Immunoreactive renal proximal and distal tubular epithelial cells in OSOM were counted visually, and the total number of renal tubular epithelial cells in OSOM in the micrographs was separately counted using the image binarization method in the Win-ROOF image analysis and measurement software (version 6.4.2., Mitani Corporation, Fukui, Japan). Then, the percentage of total immunoreactive cells was estimated in each animal.

Real-time RT-PCR analysis

To investigate the expression levels of representative cell cycle-related genes in the area of OSOM, mRNA expression analysis was performed using the StepOnePlus™ Real-time RT-PCR System (Life Technologies, Carlsbad, CA, USA) with the SYBR®Green PCR Master Mix (Life Technologies). The forward and reverse primers listed in Supplementary Table 2 were designed using the Primer Express 3.0 software (Life Technologies). Using the threshold cycle values of actin, beta (*Actb*) or glyceraldehyde 3-phosphate dehydrogenase (*Gapdh*) in the same sample as the endogenous control, the relative differences in gene expression were calculated using the $2^{-\Delta\Delta C_T}$ method (Livak and Schmittgen, 2001).

Statistical analysis

All data are represented as mean ± S.D. Numerical data were analyzed by the Bartlett's test for the homogeneity of variance. If there was no significant difference in variance, Dunnett's test was performed for comparison between the groups. If a significant difference was found in variance, Steel's test was performed. All numerical data of the treatment groups were compared with those of untreated controls.

RESULTS

Body and kidney weights

At day 3, the final body weights were significantly decreased in the NFT, TCP, and CP groups compared with untreated controls (Table 1). The absolute kidney weight of rats in the CP group was significantly lower than that of untreated controls. The relative kidney weights of rats in the NFT, ADAQ, TCP, and CP groups were significantly higher than that of untreated controls.

At day 7, the final body weights were significantly decreased in the NFT, TCP, and CP groups compared with untreated controls (Table 1). The absolute kidney weights of rats in the NFT, TCP, CP, and TAT groups were significantly lower than that of untreated controls. The relative kidney weights of rats in the NFT, TCP, and CP groups were significantly higher than that of untreated controls.

At day 28, the final body weights were significantly decreased in the NFT, TCP, and CP groups compared with untreated controls (Table 1). The absolute kidney weights of rats in the NFT and CP groups were significantly lower than that of untreated controls. The relative kidney weights of rats in the NFT, ADAQ, TCP, CP, and CBX groups were significantly higher than that of untreated controls.

Table 1. Initial and final body weights and kidney weight of rats after treatment with renal carcinogens, or non-carcinogenic renal toxicants.

Group	Number of animals	Initial body weight (g)	Final body weight (g)	Kidney weight	
				Absolute (g)	Relative (g/100 g BW)
Day 3					
CONT	10	131.7 ± 8.7[a]	150.6 ± 10.1	1.22 ± 0.09	0.81 ± 0.03
NFT	11	131.1 ± 9.9	122.8 ± 11.7**	1.14 ± 0.09	0.94 ± 0.09**
ADAQ	11	130.2 ± 9.8	143.9 ± 9.2	1.25 ± 0.07	0.87 ± 0.04*
TCP	11	132.0 ± 11.4	124.5 ± 9.5**	1.19 ± 0.10	0.96 ± 0.04**
CP	10	131.9 ± 7.0	124.8 ± 7.9**	1.09 ± 0.09**	0.87 ± 0.05*
TAT	10	132.3 ± 8.5	149.1 ± 8.7	1.21 ± 0.08	0.81 ± 0.02
CBX	10	131.8 ± 6.3	148.8 ± 8.2	1.19 ± 0.08	0.80 ± 0.02
Day 7					
CONT	10	133.8 ± 8.5	176.2 ± 10.8	1.43 ± 0.08	0.81 ± 0.04
NFT	11	133.9 ± 11.7	116.9 ± 8.8**	1.12 ± 0.10**	0.96 ± 0.07**
ADAQ	11	133.3 ± 9.6	168.8 ± 11.6	1.40 ± 0.14	0.83 ± 0.03
TCP	11	134.7 ± 8.2	133.9 ± 10.7**	1.24 ± 0.10**	0.93 ± 0.03**
CP	10	135.6 ± 8.2	130.4 ± 7.0**	1.14 ± 0.10**	0.87 ± 0.04**
TAT	10	133.0 ± 10.0	168.2 ± 11.7	1.31 ± 0.13*	0.78 ± 0.03
CBX	10	132.6 ± 7.8	171.2 ± 11.3	1.35 ± 0.07	0.79 ± 0.03
Day 28					
CONT	10	118.6 ± 6.8	240.9 ± 5.7	1.66 ± 0.08	0.69 ± 0.03
NFT	11	119.5 ± 6.2	131.0 ± 9.7**	1.31 ± 0.14**	1.00 ± 0.10**
ADAQ	11	119.5 ± 6.1	228.9 ± 16.3	1.76 ± 0.13	0.77 ± 0.03**
TCP	11	121.0 ± 6.6	173.4 ± 6.4**	1.55 ± 0.07	0.89 ± 0.03**
CP	10	119.0 ± 7.4	177.1 ± 13.5**	1.54 ± 0.09*	0.87 ± 0.03**
TAT	10	119.5 ± 6.4	234.8 ± 10.8	1.61 ± 0.12	0.68 ± 0.03
CBX	10	118.9 ± 8.8	230.1 ± 13.3	1.71 ± 0.13	0.74 ± 0.02**

Abbreviations: ADAQ, 1-amino-2,4-dibromoantraquinone; CBX, carboxin; CONT, untreated controls; CP, 1-chloro-2-propanol; NFT, nitrofurantoin; TAT, triamterene; TCP, 1,2,3-trichloropropane.

[a] Values are expressed as mean ± S.D.

* $P < 0.05$, ** $P < 0.01$ vs. untreated controls (Dunnett's or Steel's test).

Histopathological changes

NFT treatment induced hyaline droplet degeneration of proximal tubules in the cortex from day 3 of treatment, and scattered proximal tubular regeneration in the cortex and OSOM at day 28. Similar to a previous report (NTP, 1996), ADAQ treatment induced hyaline droplet degeneration of proximal tubules in the cortex from day 3 of treatment, and proximal tubular pigmentation in the OSOM and scattered tubular regeneration in the cortex and OSOM at day 28. TCP treatment induced proximal tubular cell karyomegaly accompanied with diffuse regenerative hyperplasia in the OSOM from day 3, similar to previous report (NTP, 1993a). CP treatment induced marginal hyaline droplet degeneration of proximal tubules in the cortex at day 28. TAT treatment induced hyaline droplet degeneration of proximal tubules in the cortex, and scattered tubular regeneration in the cortex and OSOM at day 28, similar to previous report (NTP, 1993b). CBX treatment induced scattered tubular regeneration in the cortex and OSOM, and hyaline cast in the Henle's thin segment and collecting tubules, accompanied with diffuse regeneration of collecting tubules at day 28.

Distribution of immunoreactive cells and apoptotic cells

Ki-67, p-Histone H3, TOP2A, and p-MDM2 were immunolocalized in the nucleus of tubular epithelial cells, and UBD was immunolocalized in the cytoplasm or mitotic spindle of tubular epithelial cells (Figs. 1-3). TUNEL$^+$ apoptotic cells were also observed in tubular epithelial cells (Figs. 1-3). Ki-67$^+$, p-Histone H3$^+$, TOP2A$^+$, UBD$^+$, and TUNEL$^+$ cells were evenly distributed in the renal tubules within the kidney. With regard to p-MDM2, immunoreactive cells were predominantly observed in distal tubular epithelial cells.

At day 3, the number of Ki-67$^+$ cells significantly increased in the NFT, TCP, and CBX groups, and significantly decreased in the ADAQ and TAT groups compared with untreated controls (Fig. 1A). The number of p-Histone H3$^+$ cells significantly increased in the NFT and TCP groups, and significantly decreased in the TAT group compared with untreated controls (Fig. 1B). The number of TOP2A$^+$ cells significantly increased in the NFT, TCP, CP, and CBX groups, and significantly decreased in the ADAQ and TAT groups compared with untreated controls (Fig. 1C). The number of UBD$^+$ cells significantly increased in the NFT, TCP, and CBX groups, and significantly decreased in the ADAQ and TAT groups compared with untreated controls (Fig. 1D). The number of p-MDM2$^+$ cells significantly decreased in the NFT, ADAQ, TCP, CP, and TAT groups compared with untreated controls (Fig. 1E). The number of TUNEL$^+$ cells did not change in any of the treatment groups (Fig. 1F).

At day 7, the number of Ki-67$^+$ cells significantly increased in the NFT and TCP groups, and significantly decreased in the ADAQ and TAT groups compared with untreated controls (Fig. 2A). The number of p-Histone H3$^+$ cells significantly increased in the NFT group, and significantly decreased in the CP group compared with untreated controls (Fig. 2B). The number of TOP2A$^+$ cells significantly increased in the TCP group, and significantly decreased in the ADAQ and TAT groups compared with untreated controls (Fig. 2C). The number of UBD$^+$ cells significantly increased in the TCP group, and significantly decreased in the ADAQ and TAT groups compared with untreated controls (Fig. 2D). The number of p-MDM2$^+$ cells did not change in any of the treatment groups (Fig. 2E). The number of TUNEL$^+$ cells significantly increased in the NFT and TCP groups compared with untreated controls (Fig. 2F).

At day 28, the number of Ki-67$^+$ cells significantly increased in the NFT, ADAQ, TCP, and CBX groups compared with untreated controls (Fig. 3A). The number of p-Histone H3$^+$ cells significantly increased in the NFT and CBX groups compared with untreated controls (Fig. 3B). The number of TOP2A$^+$ cells significantly increased in the ADAQ, TCP, and CBX groups compared with untreated controls (Fig. 3C). The number of UBD$^+$ cells significantly increased in the ADAQ, TCP, and CBX groups compared with untreated controls (Fig. 3D). The number of p-MDM2$^+$ cells significantly increased in the TCP group, and significantly decreased in the NFT and CP groups compared with untreated controls (Fig. 3E). The number of TUNEL$^+$ cells significantly increased in the CBX group compared with untreated controls (Fig. 3F).

p-Histone H3$^+$/Ki-67$^+$ cell ratio

To estimate the number of proliferative cells existing at M phase, the ratio of the number of p-Histone H3$^+$ cells to that of Ki-67$^+$ cells was calculated using data obtained from kidney slides immunohistochemically stained for each molecule in the same animal.

At day 3, the ratio of the number of p-Histone H3$^+$ cells to that of Ki-67$^+$ cells significantly decreased in the TCP group compared with the untreated controls (Fig. 4A). At day 7, the ratio of the number of p-Histone H3$^+$ cells to that of Ki-67$^+$ cells significantly decreased in the TCP group compared with untreated controls (Fig. 4B). At day 28, the ratio of the number of p-Histone H3$^+$ cells to that of Ki-67$^+$ cells significantly decreased in the ADAQ and TCP groups compared with the untreated controls (Fig. 4C).